A general effective approach to the synthesis of shaped beams for arbitrary fixed-geometry arrays

SUBMISSION TEMPLATE FOR JOURNAL OF ELECTROMAGNETIC WAVES AND APPLICATIONS

A General Effective Approach to the Synthesis of Shaped Beams for Arbitrary Fixed-Geometry Arrays

Giada M. Battaglia[a], Gennaro G. Bellizzi [a,b], Andrea F. Morabito[a] ,Gino Sorbello[c] and Tommaso Isernia[a]

[a]Department of Information, Infrastructure and Sustainable Energy Engineering, Università Mediterranea di Reggio Calabria, via Graziella Località Feo di Vito, 89122 Reggio Calabria, Italy;
[b]Department of Radiation Oncology, Erasmus University Medical Center, Dr. Molewaterplein 40, 3015 GD, Rotterdam, The Netherlands;
[c]Department of Electrical, Electronic and Computer Engineering, Università di Catania, Viale Andrea Doria 6, 95125 Catania, Italy.

ARTICLE HISTORY
Compiled July 8, 2019

ABSTRACT
We propose a new approach to the mask-constrained synthesis of shaped beams through generic array antennas having arbitrary layouts and element patterns. The introduced general methodology allows casting the design problem as a finite number of Convex Programming optimizations and can generate different excitation solutions all fulfilling the required specifications. Numerical examples, including planar arrays and the full-wave synthesis of an aperiodic array, are provided in support of the given theory.

KEYWORDS
Antenna pattern synthesis, array antennas, convex programming, shaped beams.

1. Introduction

Shaped-beam pattern synthesis is of interest in many antenna applications, as shown by the large number of classical (e.g.,[1–7]) and up-to-date (e.g.,[8–20]) contributions.

A very popular approach has been given by Woodward and Lawson (WL) in [6]. In the latter, the shaped pattern is conceived as the superposition of many pencil beams which are steered and then summed in such a way to achieve the desired shaping. While being intuitive and straightforward, the WL method suffers from a number of relevant drawbacks. In fact, as already noticed in [7], it does not guarantee the full control of the field in the shaped-beam zone in case of severe constraints. Moreover, the synthesized field is restricted within the class of real patterns, so that one is not exploiting all the degrees of freedom of the problem.

By taking inspiration from [7], an approach similar to the WL technique has been recently proposed in [9], wherein Taylor beams are superimposed in order to gener-

CONTACT Andrea F. Morabito. Email: andrea.morabito@unirc.it

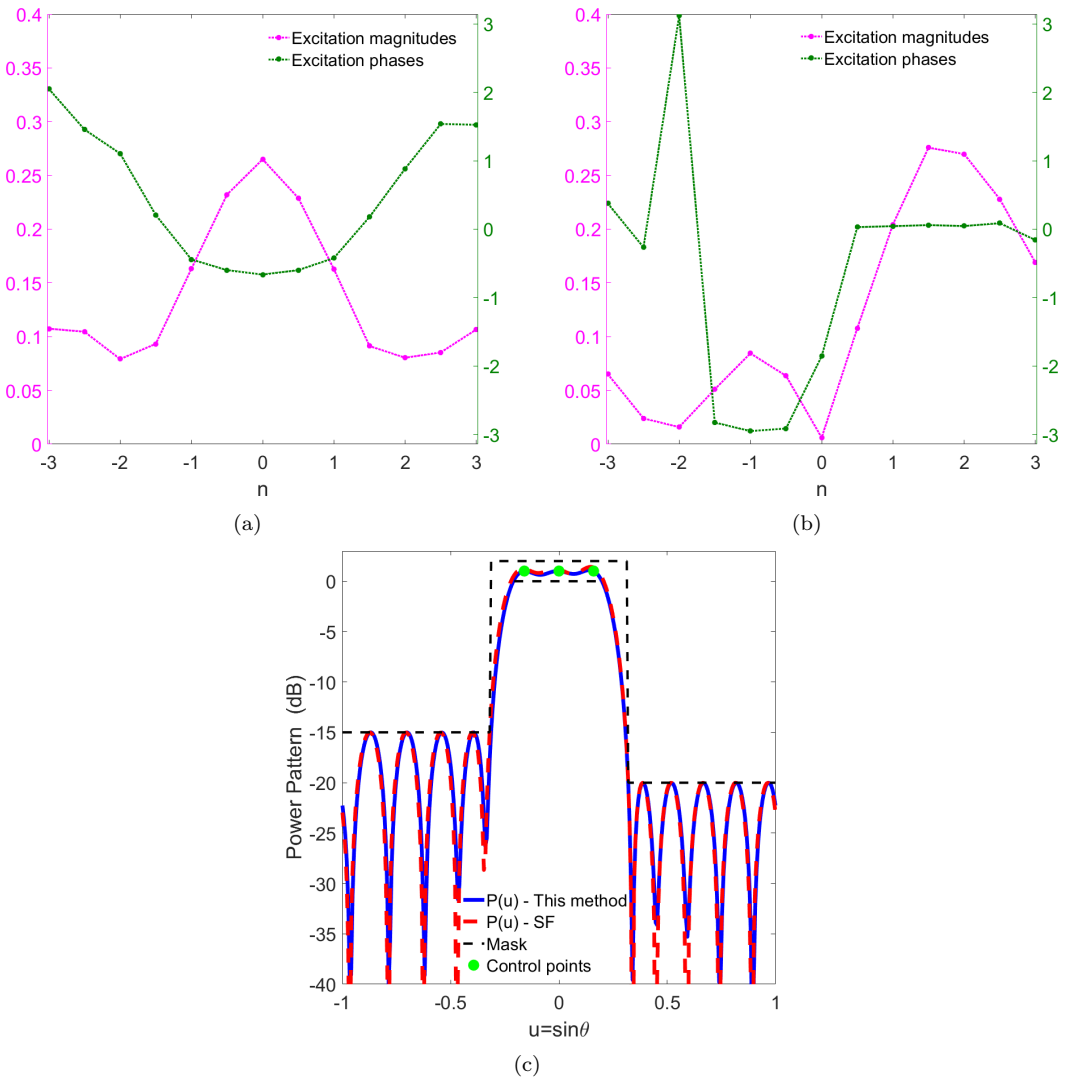

Figure 1. First synthesis problem of Subsection 3.1. Two different excitation sets synthesized through the proposed method [(a) and (b)] and square-amplitude far-field distribution [denoted from now on by *P(u)*] corresponding to both of them (c): flat-top beam provided by the proposed procedure (blue line) as well as by the approach in [4] (red line), and adopted mask (black line).

ate the desired pattern. This approach allows some improvements in the control of sidelobes. Unfortunately, it still does not guarantee their full oversight. Moreover, and more important, the resulting patterns are still real, so that not all degrees of freedom are exploited. Therefore, the approach is affected by essentially the same limitations inherent to the WL method.

A more general approach relies on the so-called 'semidefinite relaxation' framework [14]. In fact, it allows dealing with generic (fixed-geometry) arrays. On the other side, in this technique the number of unknowns exhibits a quadratic grown with the number of array elements, thus possibly implying serious computational problems. Moreover, at the end of the procedure only one solution can be found, so that a number of potentially-interesting solutions are lost.

Computational burden issues again come into play whenever the synthesis is tackled (as for instance in [8]) by recurring to global optimizers.

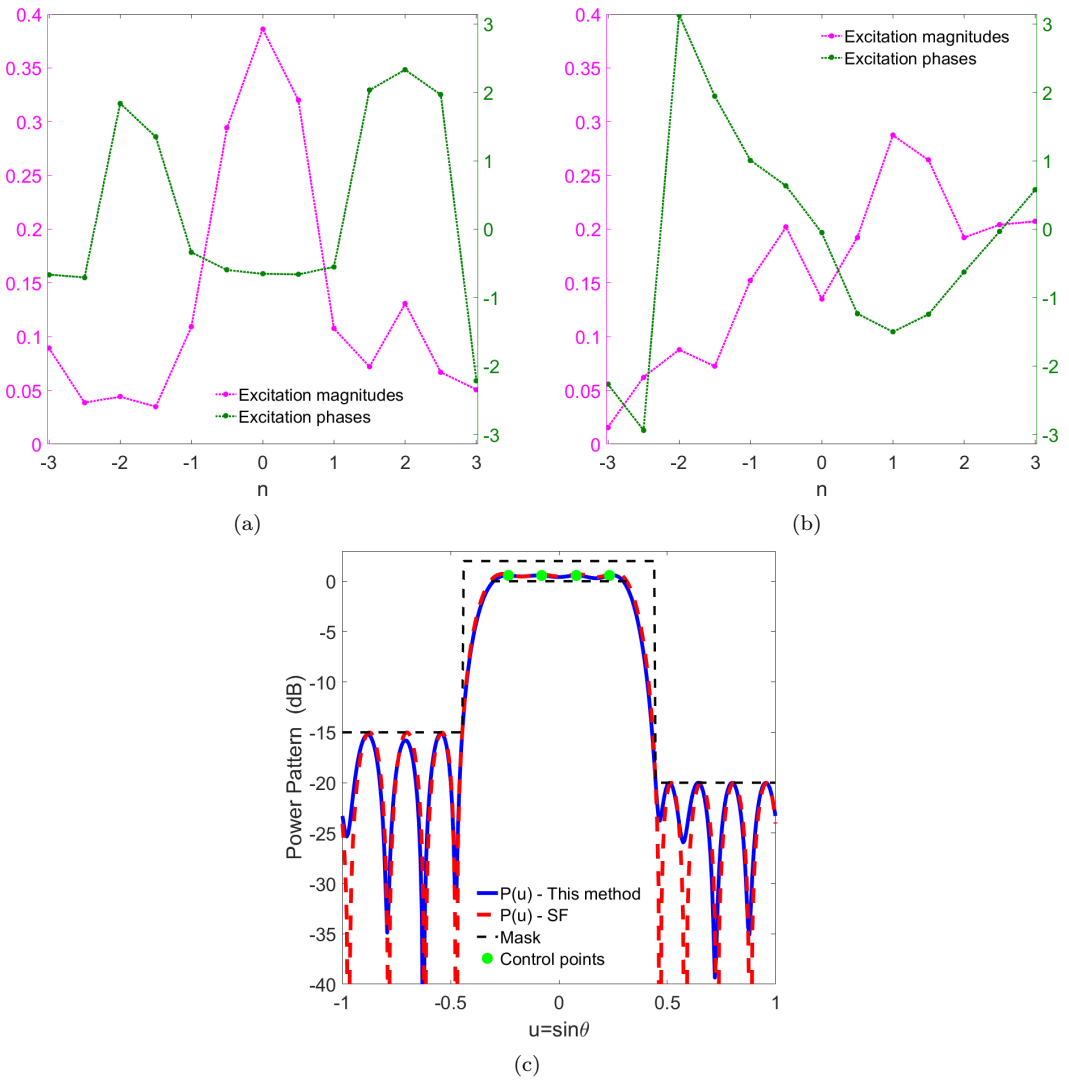

Figure 2. Same as Fig. 1, but now with reference to the second synthesis problem dealt with in Subsection 3.1.

A very powerful approach which presents none of the above drawbacks is the Spectral Factorization (SF) method, which has been proposed for the first time to array synthesis in [3] and then, in a more widespread fashion, in [4] and [5]. Notably, this technique allows casting the synthesis as a mask-constrained one while still being computationally effective and not recurring to undesired limitations on the degrees of freedom. From the operative point of view, the array design is performed as a Linear Programming (LP) problem plus a polynomial factorization, with relevant advantages in terms of computational burden and global optimality of solutions. Moreover, the approach is able to find all the different possible solutions to the problem at hand, so that the designer can choose the most-convenient one according to some quality parameter. By taking advantage of these results, SF has been recently exploited in the synthesis of equispaced reconfigurable arrays [17], continuous aperture sources [18] (in turn allowing the design of 1-D [15] as well as circular-ring [16] isophoric sparse arrays), and 1-D arrays having either even excitations [10] or a high beam efficiency [19].

Another benchmark and well-assessed approach is the Orchard-Elliott-Stern (OES) one [2]. While antecedent to [3–5], this technique is similar in spirit to the SF method but for optimizing the zeroes (rather than the coefficients) of the polynomial underlying the sought power pattern.

Unfortunately, both SF and OES methods can be applied in a straightforward fashion only if the far-field can be written in terms of a 1-D trigonometric polynomial, i.e., in case of either equispaced 1-D arrays with identical element patterns, or circularly-symmetric fields, or *u-v* factorable planar arrays. Such a limitation does not allow, for instance, considering 1-D arrays having an aperiodic layout and/or different elements' radiation patterns (where mounting-platform and mutual-coupling effects come into play) as well as generic planar or conformal arrays.

In the attempt of overcoming the disadvantages of the different methods recalled above, we propose in the following a completely-new approach to the mask-constrained power synthesis of shaped beams which keeps many of the SF advantages while dealing with generic fixed-geometry arrays (including sparse, conformal, and planar arrays) and taking into account mutual-coupling and mounting-platform effects. The method is related to the WL one as it also adopts several properly-spaced 'control points' located in the shaped-beam zone. On the other side, as it will be shown, similarities end here. In fact, the proposed approach is able to exploit all the degrees of freedom of the problem by looking for complex patterns. Also, it directly looks for a shaped pattern (rather than for a superposition of pencil beams). In so doing, it is able to take into account since from scratch the fulfillment of constraints on sidelobes. Moreover, similarly to the SF method, the approach allows identifying (if any) a multiplicity of substantially-different excitation sets all fulfilling the assigned power-pattern mask. The approach is also able to cast the synthesis in terms of a number of Convex Programming (CP) problems, with the inherent advantages. Finally, it can pursue patterns which cannot be expressed as the deformation of a circularly-symmetric field, e.g., requiring localized depressions or distinct beams.

In the following, the proposed technique is presented in Section II and assessed in Section III, where the numerical analysis confirms the expected advantages with respect to the above methods. Conclusions follow.

2. The Proposed Beam Shaping Approach

The component of interest of the far-field of a generic N-elements array can be written as:

$$F(\underline{r}) = \sum_{n=1}^{N} I_n \Psi_n(\underline{r}) \tag{1}$$

wherein $\underline{r}$ is the coordinate spanning the observation space, $\Psi_n(\underline{r})$ is the complex field induced by the unitary-excited *n-th* antenna in the region of interest Ω when all the other antennas are turned off, and I_n represents the complex excitation of the *n-th* element. As well known, the function $\Psi_n(\underline{r})$ represents the n-th Active Element Pattern (AEP), which takes into account possible mutual-coupling and mounting-platform effects [20].

The goal is that of determining the optimal excitations such as to grant the desired

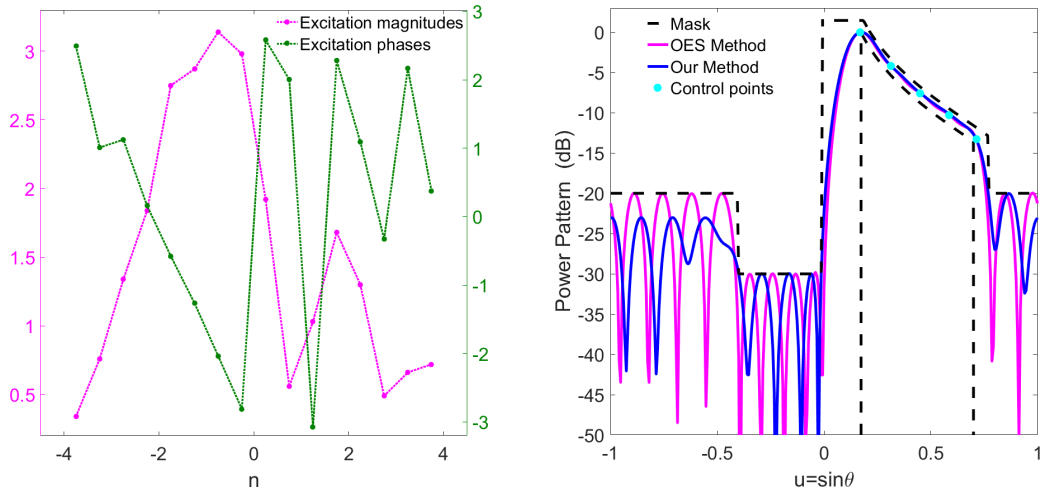

Figure 3. Comparison with [2]: excitations set synthesized through the proposed method (a) and comparison between the power pattern corresponding to them and the OES solution (b).

shape and the minimum ripple of the pattern in the 'target' region Λ while fulfilling arbitrary upper-bound constraints in the 'sidelobes' region Ω.

In order to present the proposed synthesis approach, given the array layout and $\Psi_n(\underline{r})$ for $n = 1, \ldots, N$, let us consider the sampling of Λ into L 'control points', say $\underline{r}_{\Lambda i}, i = 1, \ldots, L$. The latter should be chosen in such a way to allow the full control of the pattern in the shaped zone while not being redundant. An obvious answer to such a question is the observation that far-field patterns are bandlimited [21], so that the control points are conveniently chosen by sampling Λ at the Nyquist distance. Then, by considering $\underline{r}_{\Lambda 1}$ as a 'reference' point, i.e., as the point wherein the phase of the synthesized field is fixed (to zero) once and for all, let us indicate with $\varphi_i \in [-\pi, +\pi]$ the field phase shift between $\underline{r}_{\Lambda i}$ and $\underline{r}_{\Lambda 1}$. Under these assumptions, for any fixed determination of the phase shifts $\varphi_2, ..., \varphi_L$, one can consider the following synthesis problem:

Find the complex excitations $I_1, ..., I_n$ in such a way that:

$$\Re\{F(\underline{r}_{\Lambda i})\} = \alpha_i \cos\varphi_i \qquad i = 1, \ldots, L \tag{2.a}$$

$$\Im\{F(\underline{r}_{\Lambda i})\} = \alpha_i \sin\varphi_i \qquad i = 1, \ldots, L \tag{2.b}$$

$$\left|F(\underline{r})\right|^2 \leq UB(\underline{r}) \qquad \forall \underline{r} \in \Omega \tag{3}$$

where $\alpha_1, ..., \alpha_L$ are a-priori chosen real and positive numbers. In particular, while enforcing that the synthesized field is purely real in the first reference point[1], constraints (2) are equivalent to $\left|F(\underline{r}_{\Lambda i})\right| = \alpha_i$ and hence allow arbitrarily shaping the pattern at the control points. Also note that, once a sufficiently-fine discretization [21] is performed, constraints (3) allow enforcing arbitrary upper bounds on the sidelobes.

Notably, for fixed values of $\varphi_2, ..., \varphi_L$, constraints (2) are linear in the unknown excitations [2] while, as the left-hand members in (3) are positive semi-definite quadratic

[1]Note this does not entail any lack of generality, as it is simply equivalent to fix the phase reference.

[2]This property has been profitably exploited also in [22] wherein, however, the synthesis is carried out through

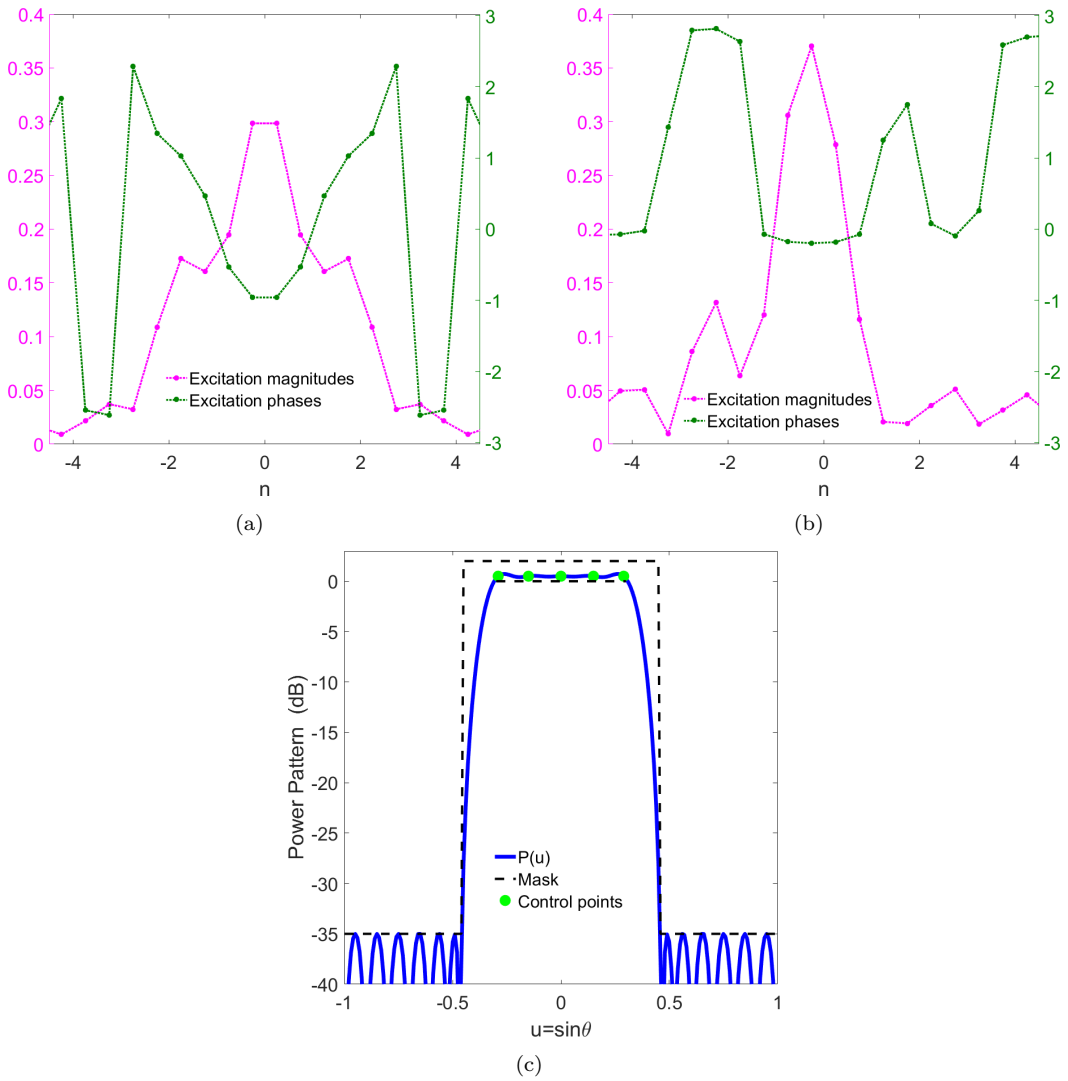

Figure 4. Comparison with [9]: two different excitation sets synthesized through the proposed method [(a) and (b)], and power pattern corresponding to both of them (c).

forms, constraints (3) define, in each discretization point, a convex set [15]. Hence, the problem (2)-(3) can be solved in a fast and effective fashion as the search for the intersection (if any) amongst convex sets. Such a feature allows us solving the overall synthesis problem through the following procedure:

i. repeatedly solve the problem (2)-(3) for different fixed values of $\varphi_2, ..., \varphi_L$;
ii. pick, amongst the instances wherein step (i) admits a solution, the one corresponding to the minimum shaped-beam ripple inside Λ.

Let us now remark the key features of the proposed method.

First, the approach is more powerful than [6] and [9] as it allows dealing with complex fields and can guarantee since from scratch the fulfillment of constraints on the sidelobes. Moreover, by using the 'reduced radiated field' concept [23], the approach

an iterative procedure which is completely different in spirit from the present approach and does not allow finding a multiplicity of solutions corresponding to the sougth power pattern.

can also be used to perform the pattern shaping on a near-field surface (rather than in the far-field zone).

Second, since different excitation sets corresponding to the same ripple can come out from step (ii), the method can allow identifying several different solutions to the problem.

Last but not least, the proposed formulation is very general. In fact, no hypotheses have been given in (1)-(3) with respect to the array's layout and AEPs so that, opposite to SF [4], OES [2], and their derivations [10,16,17,19], the procedure can be applied to whatever kind of uniformly and non-uniformly spaced linear, planar, and conformal arrays.

As a drawback, as long as enumerative techniques are used, the computational complexity of the problem increases with the number of control points as well as with the number of phase-shift instances considered for each control point. In particular, by denoting with M the number of different φ_i values considered $\forall i = 2, ..., L$ in step (i), the overall number of CP problems pertaining to step (i) will be equal to M^{L-1}. Obviously, in case of need, a smart exploitation of the space of the phase shifts (including tabu search [24] for a-priori excluding unsuitable sets of values[3], or analytical derivations for restraining the search around given values) will considerably reduce the computational burden. Also note that one can take profit from parallel computing as well as from a global optimization on phase shifts.

While having a computational complexity exponentially growing with the number of unknowns, the proposed method still implies a computational burden comparable or even lower than the one of global-optimization techniques acting on excitations (see for instance [8]) and semidefinite-relaxation approaches (see for instance [14]). In fact, global optimization also implies a computational complexity exponentially growing with the number of unknowns, but the number of elements of an array is generally much larger than the number of phase shifts to be considered. Also, approaches based on semidefinite relaxation imply a number of unknowns which quadratically grows with the number of array elements, and the relaxation from a non-convex problem to a convex one can induce non-trivial and possibly-detrimental effects.

3. Numerical Validation

In the following we report numerical examples validating the proposed technique. In particular, in order to test the approach in a case where a provably optimal procedure does exist, in Subsections A and B we provide comparisons with the SF and the OES methods. Then, in Subsection C, we show that the presented method favourable compares with the one recently proposed in [9]. Finally, in Subsections D and E, we consider instances where the OES and SF approaches cannot be applied, i.e., an aperiodic array with full-wave simulated AEPs (where the proposed technique is compared to the one in [20]) and two planar non-factorable arrays (where the outcomes are compared to the ones in [4] and [25]).

The required numerical optimizations have been performed by exploiting the *fmincon* routine of MATLAB (version R 2016b). All calculations were run on a PC equipped with the Intel i7-6700HQ processor and a 16GB RAM, with an average computational time, in 1-D test cases, equal to 0.7s per CP optimization. For each solution,

[3]For example, in the case of two control points, $\varphi_1 = \pi$ implies a negative interference at the midpoint between them, with bad effects on the ripple.

along with ripple we also evaluated the excitations' Dynamic Range Ratio, i.e.,

$$DRR = \frac{\max\limits_{n}|I_n|}{\min\limits_{n}|I_n|} \tag{4}$$

whose reduction leads to a simplification of the beam forming network and to an increase of the illumination efficiency [17].

In all experiments involving 1-D arrays we also evaluated the directivity and used the spectral variable $u = \sin\theta$ ($\theta \in [-\pi/2, \pi/2]$ denoting the angle between the observation and boresight directions) as the coordinate spanning the observation space. Consequently, the region Λ has been sampled as $u_{\Lambda 1}, ..., u_{\Lambda L}$. Finally, we considered $M = 20$ values of φ_i (uniformly-spaced in the range $[-\pi, +\pi]$).

Similarly, in the 2-D test cases, the observation space has been spanned by using the spectral variables $u = \sin\theta\cos\phi$ and $v = \sin\theta\sin\phi$ (θ and ϕ respectively denoting, this time, the usual elevation and azimuth angles with respect to the boresight). Moreover, in order to keep low the computational burden of the solution procedure, the value of M has been decreased up to 8. As it will be shown, such a reduction did not prevent the approach from achieving results which favorably compare with the literature.

3.1. Comparisons with the SF method

In this Subsection we report the outcomes of two synthesis problems wherein the proposed approach has been compared to the SF one published in [4]. To this end,we first considered the power goals depicted in Fig. 1 (c) and Fig. 2 (c), respectively, and solved them by first exploiting the SF method (wherein the ripple minimization has also been added according to the guidelines in [10]) and then by using the proposed approach. In both problems, we considered an equispaced array composed of $N = 13$ isotropic elements with a $\frac{\lambda}{2}$ inter-element spacing (λ denoting the wavelength) and set $\alpha_i = 1\ \forall i$.

In the first synthesis problem, the goal was to minimize the ripple for $u \in [-0.19, +0.19]$ (while guaranteeing anyway a maximum ripple of $\pm 1dB$) and to achieve a maximum sidelobe level lower than -15 dB for $u \leq -0.32$ and to -20 dB for $u \geq 0.32$. Fig. 1 (c) shows a comparison between the power patterns respectively achieved by exploiting the SF method and the proposed approach (wherein three equispaced control points inside the region $\Lambda \in [-0.19, +0.19]$, i.e., $u_{\Lambda 1} = -0.16, u_{\Lambda 2} = 0, u_{\Lambda 3} = 0.16$, have been used). Notably, the proposed procedure delivered exactly the same radiation performances as the SF method (corresponding to a ripple of $\pm 0.15dB$). Moreover, it turned out being able to provide multiple excitation sets giving rise to the same square-amplitude far-field distribution. Figures 1 (a) and (b) respectively depict two different excitation sets both delivering the pattern reported in Fig. 1 (c) (which provides a directivity of 6.32 dB, i.e., 0.87 dB lower than the one of a theoretical field being equal to 1 inside Λ and 0 elsewhere). For this mask, if DRR rather than ripple minimization is pursued then the DRR decreases from 3.3 to 2.7 while the ripple increases from $\pm 0.15dB$ to $\pm 0.6dB$.

In the second synthesis problem, the goal was to minimize the ripple when dealing with a broader target area, i.e., $u \in [-0.32, +0.32]$, while guaranteeing that it does not exceed $\pm 0.5dB$ and that a maximum sidelobe level lower than -15 dB for $u \leq -0.44$ and to -20 dB for $u \geq -0.44$ is achieved. Fig. 2 (c) depicts a superposition of the power patterns respectively delivered by the SF method and the proposed procedure

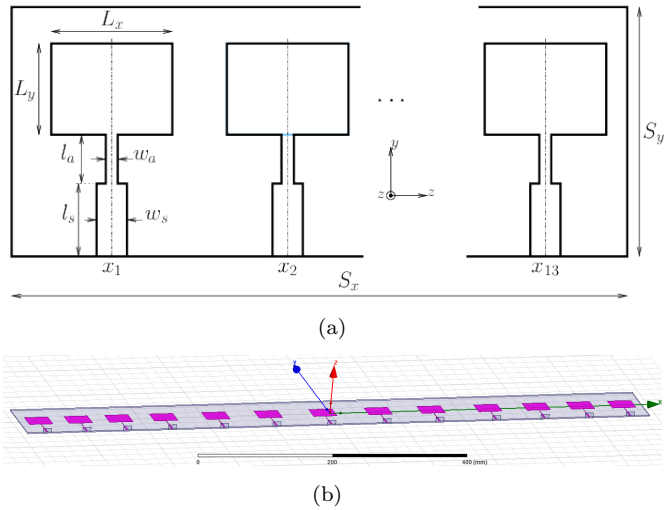

Figure 5. Unequally-spaced array designed as in Subsection 3.4: layout (a) and 3-D HFSS view (b). The key parameters of the structure are listed in Tab. 1, while the patches' locations are reported in Tab II and are the same as the ones published in [11],[13],[20].

Table 1. Radiation performances achieved by the proposed method (comparison with the technique in [2]).

Performance Parameters	OES Method	This Method
Ripple [dB]	± 0.10	± 0.14
Directivity [dB]	9.31	9.15
Max SLL for $u < 0$ [dB]	-20	-23
DRR	9.27	9.23

(wherein four equispaced control points have been set within the target area, i.e., $u_{\Lambda 1} = -0.23, u_{\Lambda 2} = -0.08, u_{\Lambda 3} = 0.08, u_{\Lambda 4} = 0.23$, and a directivity of 4.54 dB, i.e., 0.39 dB lower than the one of a theoretical field being equal to 1 inside Λ and 0 elsewhere, is provided). Results again confirm the capability of the approach to achieve radiation performances as high as those of SF (wherein the achievement of the globally-optimal solution is guaranteed), i.e., ripple=$\pm 0.06dB$, when both methods can be applied. Moreover, as in the previous example, the proposed approach has been also able to find a multiplicity of solutions. Figures 2 (a) and (b) depict two excitation sets both corresponding to the power pattern shown in Fig. 2 (c). For this mask, if DRR rather than ripple minimization is pursued then the DRR decreases from 11.1 to 6.5 while the ripple increases from $\pm 0.06dB$ to $\pm 0.36dB$.

Due to the widely-recognized effectiveness of the SF method (see for instance [10,17–19]), the results achieved in both test cases testify the good capabilities of the proposed approach. This circumstance is also corroborated by the following Subsection where, this time, the OES method will be used as a touchstone.

3.2. Comparisons with OES method

In this Subsection we challenge the proposed approach to provide performances similar to the ones achieved by the benchmark method published in [2]. To this end, we con-

Table 2. Synthesized excitations for the power pattern shown in Fig. 3 (in the same format as in [2]).

n	$\lvert I_n \rvert$	$\angle I_n$
1	0.34	-142.7°
2	0.76	-57.9°
3	1.34	-64.5°
4	1.84	-9.1°
5	2.75	33.0°
6	2.87	72.4°
7	3.14	116.7°
8	2.98	161.1°
9	1.92	-147.9°
10	0.56	-114.8°
11	1.03	176.3°
12	1.68	-130.8°
13	1.30	-62.4°
14	0.49	18.7°
15	0.66	-124.0°
16	0.72	-21.5°

Table 3. Array design parameters referring to Fig. 5.

Parameter Name	*Value [mm]*	*Description*
L_y	27.7	Patch length (resonant)
L_x	36.87	Patch width
w_a	0.5	$\lambda/4$ strip width
l_a	16.78	$\lambda/4$ adapter strip length
w_s	2.92	50 Ω strip width
l_s	15.82	50 Ω strip length
h	1.57	substrate height
S_x	978.91	substrate length
S_y	92.9	substrate width

sidered an identical radiating system (i.e., an array composed of 16 isotropic elements with a constant $\frac{\lambda}{2}$ spacing) and set the power goals as the strictest ones reported in [2]. These latter consist in enforcing for $\theta \in [10°, 50°]$ a $cosec^2(\theta) \times cos(\theta)$ power-pattern behavior and strict upper-bound constraints on the sidelobes as shown in Fig. 4 (d) of [2], where the minimum possible ripple over the main-beam region was found to be ± 0.1 dB.

To perform the synthesis, we used $L = 5$ control points, i.e., $u_{\Lambda 1} = 0.17, u_{\Lambda 2} = 0.31, u_{\Lambda 3} = 0.45, u_{\Lambda 4} = 0.59, u_{\Lambda 5} = 0.71$. Moreover, we set $\alpha_1 = 1, \alpha_2 = 0.62, \alpha_3 = 0.42, \alpha_4 = 0.31, \alpha_5 = 0.22$. The key-performance parameters achieved by one of the solutions we found are summarized (and compared to the ones of [2]) in Tab. 1, while Fig. 3 reports the achieved excitations (which are also listed in Tab. 2) and a superposition of the corresponding power pattern with the exploited mask and the OES method's best solution.

Table 4. Aperiodic arrays's element locations referring to Fig. 5 and corresponding values of Z_{Dj} and $|Z_{Dj}/Z_{jj}|$ (see also Fig. 6).

Array element	x-Position [λ]	$\lvert Z_{Dj}\rvert$ [Ω]	$\angle Z_{Dj}$ [deg]	$\lvert Z_{Dj}/Z_{jj}\rvert$
1	-3.7487	34.46	11.8	0.75
2	-3.2394	44.27	9.4	0.95
3	-2.7173	47.67	4.6	1.03
4	-2.1410	47.15	1.5	1.02
5	-1.4688	46.17	5.9	1.00
6	-0.7949	46.59	2.9	1.01
7	-0.0912	46.64	5.7	1.01
8	0.6200	45.49	4.7	0.98
9	1.3009	45.35	3.3	0.99
10	2.0304	47.91	4.1	1.03
11	2.6541	46.53	6.8	1.00
12	3.2221	41.94	-2.4	0.91
13	3.7513	43.78	1.4	0.96

Notably, the two techniques achieved very similar performances. In fact, the proposed approach allowed an improvement of both the sidelobe level (which decreased by 3 dB for $u < -0.4$ and $u > 0.9$) and the DRR (which decreased from 9.27 to 9.23) but, at the same time, provided a 0.16 dB lower directivity and a ± 0.04 dB higher ripple. Due to the well-known reliability of the OES method, these results confirm the effectiveness of the proposed approach.

3.3. Comparisons with the method recently published in [9]

We used the same reference array as in [9] (i.e., an array composed of 20 isotropic elements with a constant $\frac{\lambda}{2}$ spacing) and challenged the proposed method at lowering both the ripple value and the sidelobe level. In this case $L = 5$ control points were set within $\Lambda \in [-0.29, +0.29]$, i.e., $u_{\Lambda 1} = -0.29, u_{\Lambda 2} = -0.15, u_{\Lambda 3} = 0, u_{\Lambda 4} = 0.15, u_{\Lambda 5} = 0.29$. Moreover, we set $\alpha_i = 1 \forall i$. Fig. 4 (c) reports the synthesized power pattern (which provides a directivity of 4.76 dB, i.e., 0.6 dB lower than the one of a theoretical field being equal to 1 inside Λ and 0 elsewhere) while figures 4 (a) and (b) respectively show two different excitation sets both corresponding to it. Notably, the proposed procedure favourably compares to the one in [9] by allowing a ripple reduction from 0.25 to 0.21 dB and, at the same time, a sidelobe level reduction from -30 to -35 dB over the whole Ω region (i.e., $|u| \geq 0.45$).

3.4. Full-wave synthesis of an aperiodic array

We considered the same radiating structure and power-pattern constraints as in [20] in order to test the proposed approach in the full-wave synthesis of a non-ideal array which cannot be tackled by the SF and OES approaches. The latter is a non-uniformly spaced microstrip array composed of 13 elements (shown in Fig. 5) having the key parameters and elements' locations respectively reported in Tab. 3 and Tab. 4. The single-element coordinates are reported also in Tab. 2 of [11] and have been used also in [13] and [20]. The exploited power mask is the 'popular' square-cosecant one depicted in Fig. 6 (c) and adopted also in [1,11–13,20].

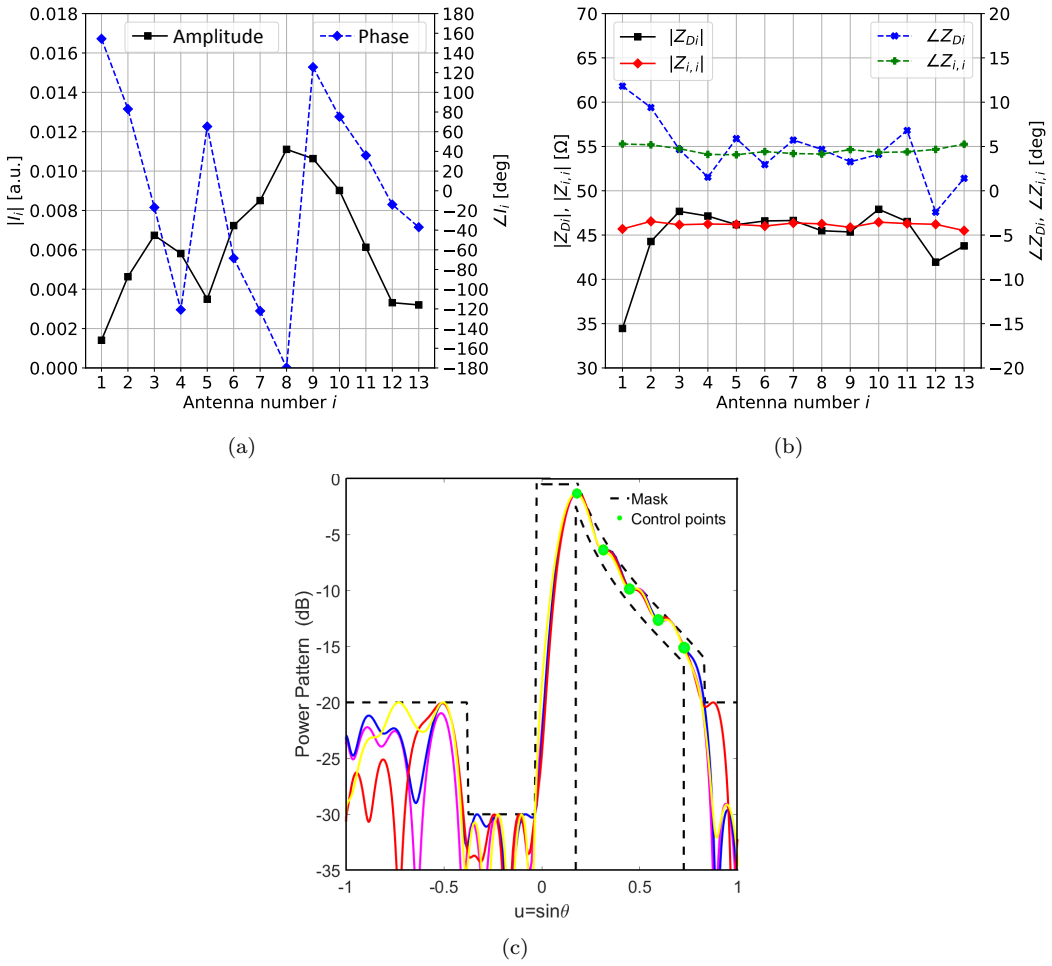

Figure 6. Synthesis of a non-uniformly spaced microstrip array (full-wave HFSS simulation, comparison with [20]): one of the achieved equivalent excitation sets (a); comparison between the active driving impedance Z_{D_i} and the self-impedance $Z_{i,i}$ of the i-th element (b); multiplicity of synthesized power patterns (c).

As a first step, we computed the AEPs through the Ansys High Frequency Structure Simulator (HFSS) full-wave software [26] by setting $f = 2.45$ GHz and discretizing the u variable into 361 points. Then, $L = 5$ control points have been uniformly set within the target area $\Lambda \in [0.17, 0.83]$, i.e., $u_{\Lambda 1} = 0.17, u_{\Lambda 2} = 0.31, u_{\Lambda 3} = 0.45, u_{\Lambda 4} = 0.59, u_{\Lambda 5} = 0.73$. In order to achieve the desired cosecant pattern the amplitude coefficients have been set $\alpha_1 = 0.86, \alpha_2 = 0.48, \alpha_3 = 0.32, \alpha_4 = 0.23, \alpha_5 = 0.17$.

Fig. 6 reports three of the synthesized power patterns (whose maximum directivity is equal, in the average, to 13.9 dB) as well as one of the corresponding excitation sets and the related active driving impedances (compared with the self-impedances). Such impedance values, which are reported also in Tab. 4, actually differ from each other. This circumstance, combined with the heterogeneity of the AEPs (which are shown in Fig. 13 of [20]), testifies the actual presence of mutual coupling. On the other hand, the element-to-element self-impedance variations are not excessive and this can lead to a simple realization of the feeding network in a standard microstrip line technology.

In this case, the minimum DRR achievable while fulfilling the power mask turned out being equal to 1.4. Notably, for identical sidelobe level performances, the proposed

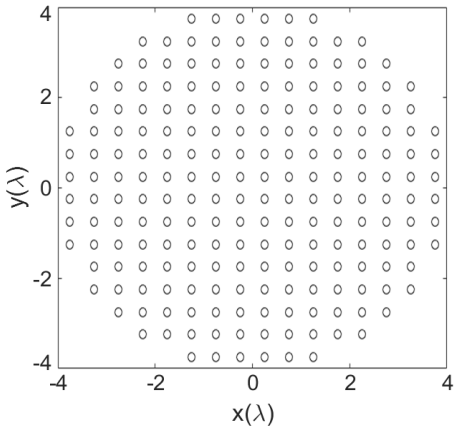

Figure 7. Layout of the array with a circular boundary used in order to compare the proposed approach to the one in [25].

approach allowed decreasing the ripple with respect to [20] from $\pm 1.25dB$ to $\pm 0.56dB$. Besides high radiation performances, the achieved results testify a feature of the approach which appears being unique, i.e., the capability of providing a multiplicity of substantially-different excitation solutions even for aperiodic non-ideal arrays whose field cannot be expressed in terms of the array factor.

3.5. Synthesis of planar arrays

In the planar arrays case, the need of a larger number of control points implies an increased computational burden. As long as the given power mask is symmetric, one can limit computational requirements by enforcing the required symmetry in the expected complex pattern (which in turn translates into linear constraints on excitations). By so doing, as shown in the following, one is able to design in a still reasonable time planar arrays composed of hundreds of elements as well as realizing fields with large footprints. Notably, although reducing the degrees of freedom available to the designer, one is still able to design array solutions which favourably compare with the literature.

To show the reliability and effectiveness of the proposed method also in the 2-D case, in the following we compare its outcomes with the ones respectively achieved by the techniques in [4] and [25] in the synthesis of two planar arrays which cannot be tackled by the SF and OES techniques.

In the first test case, we considered the same array and power mask as the one adopted in [4], i.e., a 15x15 array with isotropic elements and a constant $\frac{\lambda}{2}$ spacing as well as a mask enforcing a triangular footprint with a ripple and a peak sidelobe level respectively equal to $\pm 0.5dB$ and -29.4 dB. The enforced mask is shown in Fig. 8 (c) (as well as in Fig. 10 of [4], where the footprint's vertices are also reported). By exploiting its symmetry with respect to the spectral plane's main diagonal, it has been possible to reduce the computational complexity of the synthesis. In particular, $L = 6$ control points have been uniformly set within half of the target area, i.e., ($u_{\Lambda 1}$,$v_{\Lambda 1}$)=(-0.85,-0.85), ($u_{\Lambda 2}$, $v_{\Lambda 2}$) = (-0.25, -0.85), ($u_{\Lambda 3}$,$v_{\Lambda 3}$)=(0.34,-0.85), ($u_{\Lambda 4}$,$v_{\Lambda 4}$)=(0.85,-0.85), ($u_{\Lambda 5}$,$v_{\Lambda 5}$)=(-0.25,-0.34), ($u_{\Lambda 6}$,$v_{\Lambda 6}$)=(0.34,-0.34). Moreover, we set $\alpha_i = 1 \ \forall i$.

The square amplitude of the (complex) field synthesized through the proposed approach is shown in Fig. 8 (d) (2-D plot plus control points representation) and Fig. 8 (e) (3-D view), while figures 8 (a) and (b) report, respectively, the amplitude and phase

of the excitation sets corresponding to it. The DRR turned out being equal to 16.2. It is worth noting that the achieved power-pattern distribution perfectly agrees with the one in [4] wherein, in turn, the application of the 'feasibility criterion' guaranteed that no array with a lower number of elements can equate those radiation performances.

In the second example dealing with planar arrays, we compared the outcomes of the proposed approach to the ones shown in [25]. In that paper, the authors exploited the 208-elements circular array layout shown in Fig. 7, which was designed by starting from a 16x16 square layout (with isotropic antennas and a $\frac{\lambda}{2}$ spacing) and then discarding the locations external to the circle of radius 4λ. The resulting radiating system was aimed at generating a flat-top beam guaranteeing a ripple equal to $\pm 0.15dB$ for $|u| < 0.25$ and $|v| < 0.25$ as well as a peak sidelobe level equal to -20.6 dB for $|u| > 0.3125$ and $|v| > 0.3125$.

The adopted mask is shown in Fig. 9 (c) . In this case, its symmetry allowed us successfully performing the synthesis by looking for fields having a quadrantal symmetry. By so doing, we have been able to solve the problem by identifying just a quarter of the optimal excitations and control points. In particular, $L = 5$ control points have been uniformly set within the target area, $u, v \in [-0.25, 0.25]$, i.e., $(u_{\Lambda 1}, v_{\Lambda 1}) = (0.84, -0.08), (u_{\Lambda 2}, v_{\Lambda 2}) = (0.24, -0.24), (u_{\Lambda 3}, v_{\Lambda 3}) = (0.08, -0.08), (u_{\Lambda 4}, v_{\Lambda 4}) = (0.08, -0.24), (u_{\Lambda 5}, v_{\Lambda 5}) = (0, 0)$. Moreover, we set $\alpha_i = 1 \forall i$.

Figures 9 (d) and (e) respectively show the 2-D and 3-D plots of the power-pattern distribution associated to the synthesized (complex) field, while figures 9 (a) and (b) report, respectively, the amplitude and phase of the excitation sets corresponding to it. Notably, the proposed method favourably compares to one in [25] by allowing, for equal sidelobe level performances, a ripple reduction from $\pm 0.15dB$ to $\pm 0.1dB$ and, at the same time, a DRR reduction from 24.4 to 20.

4. Conclusions

A new general approach to the synthesis of shaped beams for generic fixed-geometry array antennas has been proposed and assessed. Differently from a large body of literature, the presented technique is not formulated in terms of global optimization of the excitations, and it allows casting the overall design as a finite number of Convex Programming optimizations. Moreover, which is a novelty with respect to all of the state-of-the-art methods, the approach allows identifying a multiplicity of excitation solutions even in those non-ideal cases where it is not possible to reason just in terms of the array factor.

The approach seems to be the first one able to grant, at the same time, all the above features plus the capability of dealing with completely-arbitrary array layouts and element patterns (including aperiodic planar and conformal arrays where mounting-platform and mutual-coupling effects are present). Notably, this is done without resorting to simplifying (yet common) assumptions such as dealing with symmetric array locations and AEPs [27], restricting the fields to the class of real ones [6,9,28], operating just in terms of the array factor [4], or pursuing (in the non-sidelobe region) a nominal-pattern synthesis rather than a mask-constrained one [6,29,30].

Results achieved in benchmark problems as well as in the case where the array factor cannot even be defined confirm the interest and validity of the approach.

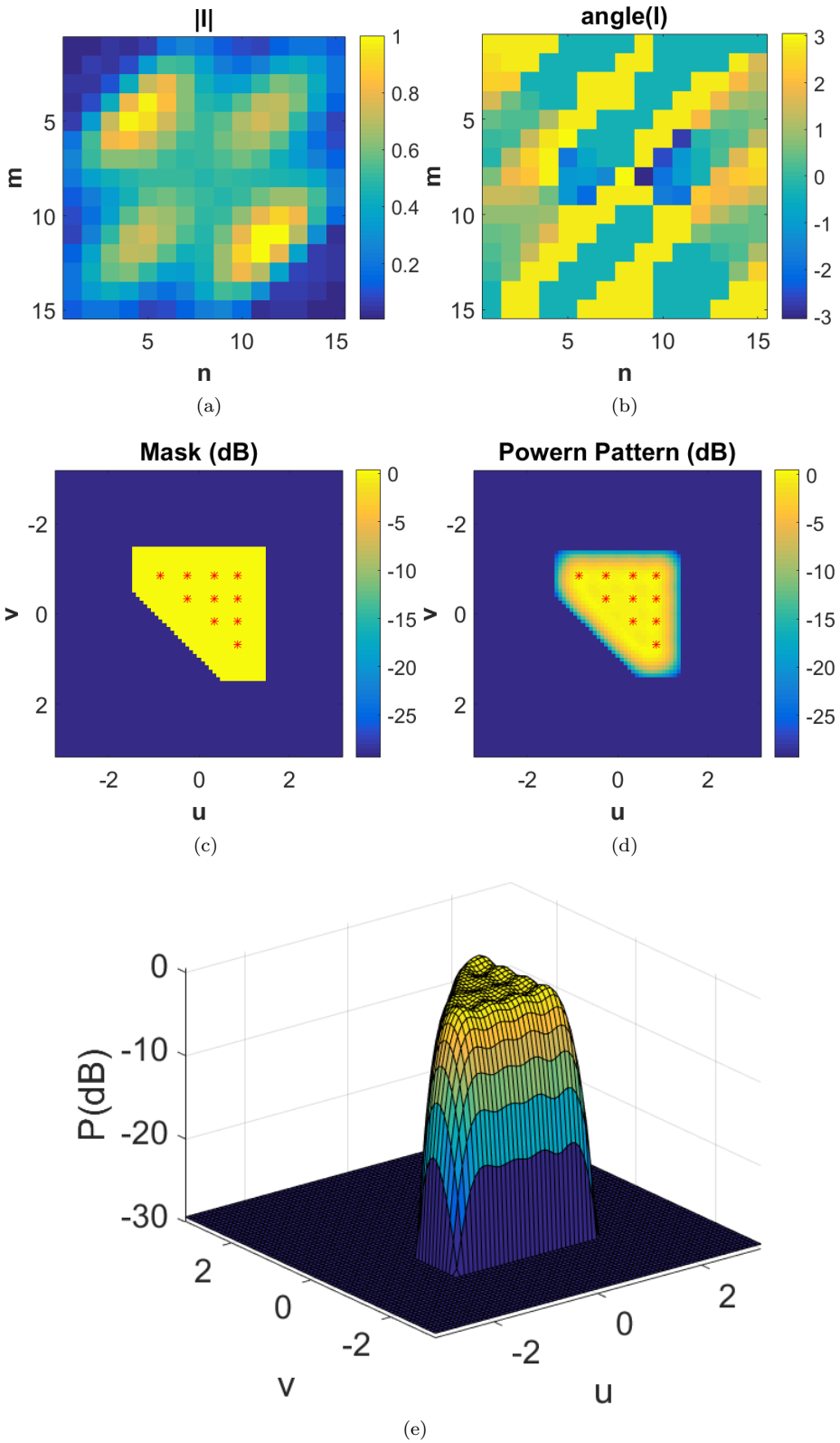

Figure 8. Synthesis of a triangular contoured beam (comparison with [4]): amplitude and phase of the excitation sets synthesized through the proposed approach [(a) and (b)]; prescribed power mask and control points (c); 2-D and 3-D power-pattern representations [(d) and (e)].

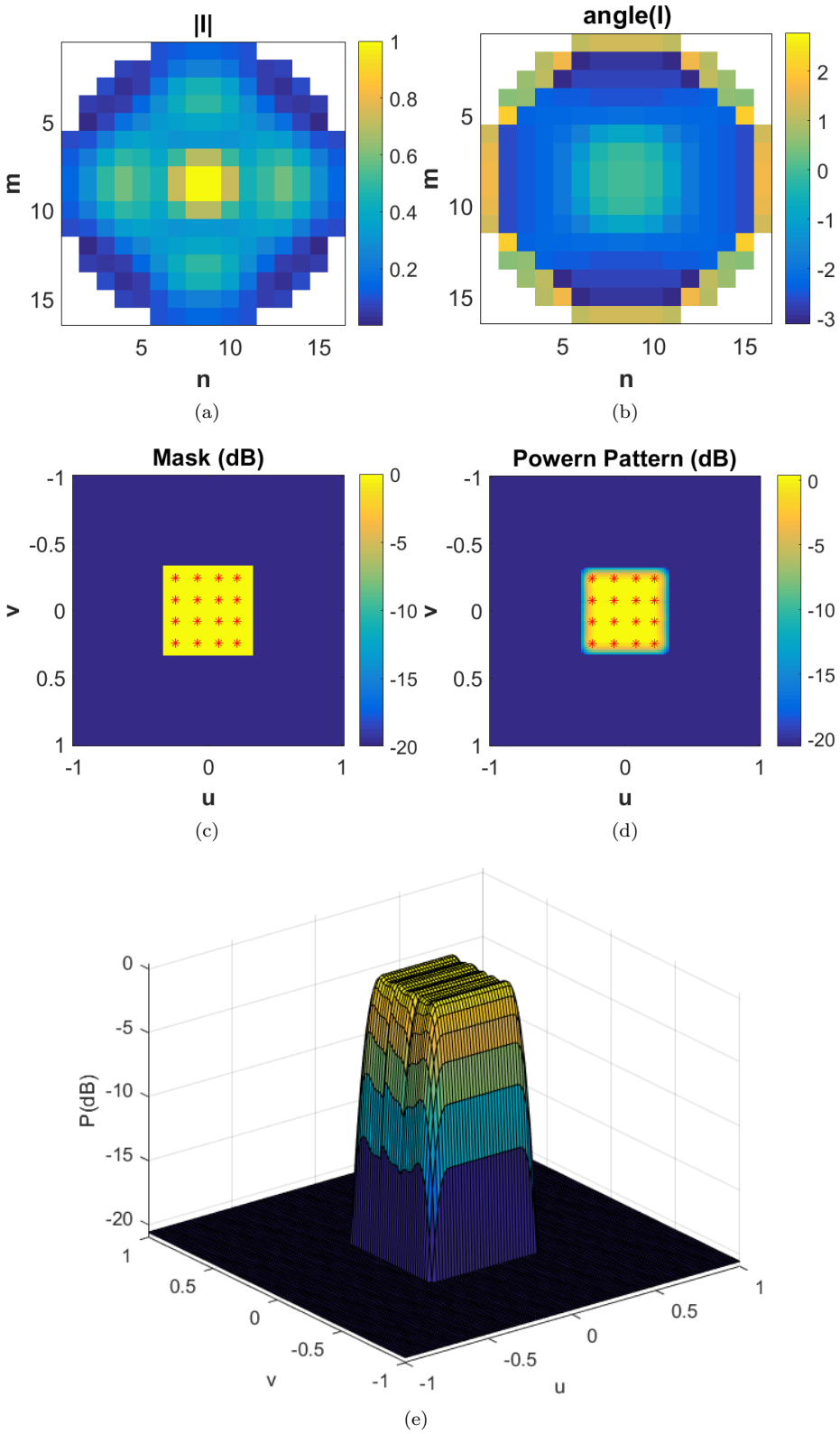

Figure 9. Synthesis of a power pattern having a large square footprint (comparison with [25]): Amplitude and phase of the excitation sets synthesized through the proposed approach [(a) and (b)]; prescribed mask and control points (c); 2-D and 3-D views of the achieved power pattern [(d) and (e)].

References

[1] R. Elliott and G. Stern. A new technique for shaped beam synthesis of equispaced arrays. *IEEE Transactions on Antennas and Propagation*, 32(10):1129–1133, 1984.

[2] H. J. Orchard, R. S. Elliott, and G. J. Stern. Optimising the synthesis of shaped beam antenna patterns. In *IEE Proceedings H (Microwaves, Antennas and Propagation)*, volume 132, pages 63–68. IET, 1985.

[3] T. Isernia. Problemi di sintesi in potenza: criteri di esistenza e nuove strategie. In *Proc. X Riunione di Elettromagnetismo*, pages 533–536, 1994.

[4] T. Isernia, O. M. Bucci, and N. Fiorentino. Shaped beam antenna synthesis problems: Feasibility criteria and new strategies. *Journal of Electromagnetic Waves and Applications*, 12(1):103–138, 1998.

[5] S. P. Wu, S. Boyd, and L. Vandenberghe. Fir filter design via spectral factorization and convex optimization. In *Applied and Computational Control, Signals, and Circuits*, pages 215–245. Springer, 1999.

[6] P. M. Woodward and J. D. Lawson. The theoretical precision with which an arbitrary radiation-pattern may be obtained from a source of finite size. *Journal of the Institution of Electrical Engineers-Part III: Radio and Communication Engineering*, 95(37):363–370, 1948.

[7] R. S. Elliott. Criticisms of the woodward-lawson method. *IEEE Antennas and Propagation Society Newsletter*, 30(3):43–43, 1988.

[8] D. W. Boeringer and D. H. Werner. Particle swarm optimization versus genetic algorithms for phased array synthesis. *IEEE Transactions on antennas and propagation*, 52(3):771–779, 2004.

[9] J. Y. Li, Y. X. Qi, and S. G. Zhou. Shaped beam synthesis based on superposition principle and taylor method. *IEEE Transactions on Antennas and Propagation*, 65(11):6157–6160, 2017.

[10] T. Isernia and A. F. Morabito. Mask-constrained power synthesis of linear arrays with even excitations. *IEEE Transactions on Antennas and Propagation*, 64(7):3212–3217, 2016.

[11] Y. Liu, Z. P. Nie, and Q. H. Liu. A new method for the synthesis of non-uniform linear arrays with shaped power patterns. *Progress In Electromagnetics Research*, 107:349–363, 2010.

[12] Y. Liu, Q. H. Liu, and Z. Nie. Reducing the number of elements in the synthesis of shaped-beam patterns by the forward-backward matrix pencil method. *IEEE Transactions on Antennas and Propagation*, 58(2):604–608, 2010.

[13] B. Fuchs. Synthesis of sparse arrays with focused or shaped beampattern via sequential convex optimizations. *IEEE Transactions on Antennas and Propagation*, 60(7):3499–3503, 2012.

[14] B. Fuchs. Application of convex relaxation to array synthesis problems. *IEEE Transactions on Antennas and Propagation*, 62(2):634–640, 2014.

[15] O. M. Bucci, T. Isernia, and A. F. Morabito. An effective deterministic procedure for the synthesis of shaped beams by means of uniform-amplitude linear sparse arrays. *IEEE Transactions on Antennas and Propagation*, 61(1):169–175, 2013.

[16] A. F. Morabito and P. G. Nicolaci. Optimal synthesis of shaped beams through concentric ring isophoric sparse arrays. *IEEE Antennas and Wireless Propagation Letters*, 16:979–982, 2017.

[17] A. F. Morabito, A. Massa, P. Rocca, and T. Isernia. An effective approach to the synthesis of phase-only reconfigurable linear arrays. *IEEE Transactions on Antennas and Propagation*, 60(8):3622–3631, 2012.

[18] O. M. Bucci, T. Isernia, and A. F. Morabito. Optimal synthesis of circularly symmetric shaped beams. *IEEE Transactions on Antennas and Propagation*, 62(4):1954–1964, 2014.

[19] A. F. Morabito. Synthesis of maximum-efficiency beam arrays via convex programming and compressive sensing. *IEEE Antennas and Wireless Propagation Letters*, 16:2404–

2407, 2017.

[20] Y. Liu, X. Huang, K. Da Xu, Z. Song, S. Yang, and Q. H. Liu. Pattern synthesis of unequally spaced linear arrays including mutual coupling using iterative fft via virtual active element pattern expansion. *IEEE Transactions on Antennas and Propagation*, 65(8):3950–3958, 2017.

[21] O. M. Bucci, C. Gennarelli, and C. Savarese. Representation of electromagnetic fields over arbitrary surfaces by a finite and nonredundant number of samples. *IEEE Transactions on Antennas and Propagation*, 46(3):351–359, 1998.

[22] K. M. Tsui and S. C. Chan. Pattern synthesis of narrowband conformal arrays using iterative second-order cone programming. *IEEE Transactions on Antennas and Propagation*, 58(6):1959–1970, 2010.

[23] O. M. Bucci and M. D'urso. Power pattern synthesis of given sources exploiting array methods. *The Second European Conference on Antennas and Propagation, Edinburg, UK, 11-16 Nov. 2007*.

[24] S. L. Ho and S. Yang. Multiobjective synthesis of antenna arrays using a vector tabu search algorithm. *IEEE Antennas and Wireless Propagation Letters*, 8:947–950, 2009.

[25] A. Rodriguez, R. Munoz, H. Estevez, F. Ares and E. Moreno. Synthesis of planar arrays with arbitrary geometry generating arbitrary footprint patterns. *IEEE transactions on antennas and propagation*, 52(9):2484–2488, 2004.

[26] *Ansoft High Frequency Structural Simulator (HFSS), Ver. 13, Ansoft Corp., Pittsburgh, PA, USA*, 2010.

[27] G. Bellizzi and O. M. Bucci. On the Optimal Synthesis of Sum or Difference Patterns of Centrosymmetric Arrays Under Arbitrary SideLobe Constraints. *IEEE Transactions on Antennas and Propagation*, 66(9):4620–4626, 2018.

[28] T. Zhang and W. Ser. Robust beampattern synthesis for antenna arrays with mutual coupling effect. *IEEE Transactions on Antennas and Propagation*, 59(8):2889–2895, 2011.

[29] Thompson J. S. Cao, P. and H. Haas. Constant modulus shaped beam synthesis via convex relaxation. *IEEE Antennas and Wireless Propagation Letters*, 16:617–620, 2016.

[30] B. Fuchs. Shaped beam synthesis of arbitrary arrays via linear programming. *IEEE antennas and wireless propagation letters*, 9:481–484, 2010.